SCHOOL OF ELECTRICAL ENGINEERING
AND TELECOMMUNICATIONS

Resource Allocation for Distributed SWIPT-enabled Secure Communication Systems

by

Jiawang Zeng

Thesis submitted as a requirement for the degree of

Master of Engineering (Telecommunication Engineering)

Submitted: Nov. 27, 2022

Abstract

The main purpose of resource allocation of distributed antenna multi-point coordination SWIPT system is to reduce the system power consumption and to improve communication security. Considering that there are two types of receivers, malicious eavesdroppers (Eve), and energy harvesting users (EH) are potential eavesdroppers, the distributed radio head adopts a cooperative approach to achieve the goal through artificial noise and beamforming technology. The problem is formulated as a non-convex problem of positive semi-definite programming, that facilities the development of a computationally efficient suboptimal algorithm based on successive convex approximation of SCA with polynomial complexity.

Keywords—- Non-convex algorithm, beamforming, multi-point coordination network, SWIPT, optimization.

Acknowledgements

I am grateful to everyone who have provided feedbacks on the writing of this thesis. In particular my supervisor Dr. Derrick Wing Kwan Ng, his passion for academics positively has influenced me.

Abbreviations

SWIPT Simultaneous Wireless Information and Power Transfer

WPT Wireless Power Transfer

CoMP Multi-point coordinated

RRH Remote radio head

SDP Semidefinite programming

SDR Semidefinite relaxation

MIMO Multiple-Input Multiple- Output

TS Time splitting

IR Information receiver

ER Energy receiver

EH Energy harvesting

Eve Eavesdropper

CP Central processor

QCQPs Quadratically constrained quadratic programming

Contents

Chapter 1

Introduction

The worldwide telecommunications industry consumed 354 TWh of electricity annually in 2012 compared to 219 TWh in 2007, according to a study by Aris and Shabani [1]. From 2013 through 2018, the consumption rate is anticipated to increase by an additional 10% annually. As a result, the operating expenses (OPEX) have climbed dramatically because electricity costs account for a sizable amount of OPEX. The huge rise in energy consumption in the communications industry is primarily due to cellular networks [2, 3]. To satisfy the expectations of mobile customers, network operators have been prompted to construct more base stations due to the rapidly growing in mobile subscribers and data traffic [4]. Cellular networks have developed remarkably and are now capable of meeting user needs. Researchers have concentrated on Green Networking and Communications to provide energy-saving options for next-generation wireless communication standards to address the problem of increasing power usage [5]. As a result, current research in both business and academia has focused heavily on energy-efficient system designs [6, 7].

Future automobiles will come with a variety of sensors, which makes it complicated to repeatedly replace the battery or replenish energy to address this critical issue, WPT technology has been proposed [8]. In practice, this technology provides energy to equipment through radio frequency signals, which can achieve the purpose of a controllable wireless energy supply [9]. According to [10], a system that uses wireless power to provide energy for information transmission and reception is defined.

In addition, massive devices will be widely used in future IoT networks to accomplish connectivity. By 2020, it's anticipated that more than 20.4 billion wirelessly linked gadgets to the Internet [11]. Green IoT has encountered challenges due to the device's short battery capacity, high power costs, and limited spectrum resources [12]. SWIPT allows customers' connectivity to continue operating even in the event of a device battery shortage, allowing for the flow of information [12]. On the one hand, SWIPT allows the device's life to be successfully prolonged while maintaining quality service (QoS) by adopting radio frequency energy. Combining the above two points, because of constantly rising energy consumption and the continuing rise in carbon dioxide emissions, green energy saving has inevitably become a problem that should be considered. Indeed, the problem is more pronounced in SWIPT systems as it requires high-power radiation for effective WPT [13].

As wireless technology rapidly expands, information security has become important. Although the traditional application layer encryption method can solve the information leakage problem, the shortcomings of this method are obvious, for instance, the requirement to share secret keys and the difficulty of the calculation. Instead, physical layer security becomes a practical solution that takes advantage of physical channel fading and interference to accomplish safe communication [14, 15, 16].To achieve physical layer security, beamforming techniques can be adopted [17], or artificial noise can be introduced into the null space spent by the receiver channels through additional spatial degrees of freedom of the antenna This can significantly reduce the QoS for eavesdroppers[18]. However, to ensure safe communication, a substantial percentage of transmit power is dedicated to emitting artificial noise [19, 20].

On the other hand, for directional signal transmission or reception in sensor arrays, beamforming or spatial filtering is a signal processing method. This is accomplished by strategically placing components in an antenna array so that some signals interfere constructively while others interfere destructively. Beamforming enables spatial selectivity. The directivity of the array refers to the enhancement over omnidirectional reception and transmission [21]. This approach can improve service quality, reduce interference, and increase security.

Furthermore, in [22], for the purpose of lowering the system's transmit power, the authors considered the coordinated multipoint (CoMP) SWIPT system, which is a crucial technology for enhancing spectral efficiency, increasing system coverage, and reducing interference. In addition, they designed a structure that exploits the central processing unit to control the remote radio head (RRH). They assign computationally intensive and energy-intensive tasks to CPU processing, while the RRH performs RF-related functions, such as amplification and filtering. The backhaul link is adopted by the RRH to connect to the CP, which might be a local high-performance processor or a cloud computing network. This effectively combats path loss and shadow attenuation. The comprehensive cooperation of CoMP can reduce energy costs effectively. The CoMP system's backhaul capacity is, however, often constrained. Consideration must be given to resource allocation in the event that backhaul capacity is constrained.

To sum up, the next-generation communication system and IoT system urgently need a means that can reduce energy consumption and ensure communication security. The system combining CoMP distributed antenna with beamforming and artificial noise technology will achieve this goal.

We design a challenge to reduce the power usage of distributed antenna multipoint coordination SWIPT systems while taking into account physical layer security. The system implements beamforming techniques as well as artificial noise to reduce the SINR of a potential eavesdropper such that it is unable to decode the desired information. This problem is defined as a non-convex problem. In contrast to convex optimization, we lack a useful set of tools for tackling non-convex problems, which makes them challenging. It is known that many nonconvex optimization problems are NP-hard. A number of non-convex issues that are challenging to both estimate and solve optimally make the situation even more hopeless [23]. Fortunately, we rephrase the problem by substituting convex deterministic requirements for the non-convex probability constraints. A semidefinite programming (SDP) relaxation approach is then exploited to get the optimal solution [24]. Furthermore, we provide a polynomial complexity iterative technique based on repeated convex approximations to overcome the issue and produce a suboptimal resource allocation strategy.

Chapter 2

Literature Review

2.1 Background

Various studies in recent years have shown that the SWIPT systems can support the explosive growth of wireless communication devices [25, 26, 27], as well as the emerging low-power IoT systems, sensor networks, and backscatter tags. In the past decades, energy prices are increasing rapidly, such that green energy saving in communication systems has become more important. Hence SWIPT's optimal beamforming to achieve the lowest power consumption design has become very valuable. On the other hand, distributed antennas have huge advantages over single-antenna base stations. Indeed distributed antenna offers special diversity that shortens the path loss, and the transmit power. Furthermore, with the growth of wireless devices, information security is threatened, because the probability of users being eavesdropped on increases, and methods to achieve physical layer security through artificial noise are proposed [15, 18]. Therefore, designing communication systems that reduce energy consumption and improve communication security becomes a time crunch.

2.2 Wireless Communication Systems

The future of mobile communications is anticipated to be considerably different from what it is right now. In order to power the future generation of wireless communication systems, energy harvesting (EH) from external power sources is a necessity due to the high-quality video and greater widescreen resolutions in mobile devices. The next telecom standard after the 4G/IMT advanced standard is the 5G [25]. By the time the first 5G standard is predicted to be ready for exploitation, there will likely be hundreds of billions or maybe trillions of linked devices due to the numerous new applications for personal communications [25, 28]. The first generation of analog communication technology was proposed in 1982. This is a summary of the journey of several generations of cellular networks. Digital communication is the cornerstone of the second generation (2G), which was first presented in 1991. Furthermore, 2G introduced cellular data via the GPRS. Third-generation (3G) networks, which offer greater data rates than 2G, were introduced over ten years later. The fourth generation of communications (4G), with higher data rates and more sophisticated technology, was released about ten years later. In particular, 5G wireless communications are anticipated to significantly decrease latency and energy usage while increasing data speeds, capacity, coverage, and connection dependability [29].

2.3 Wireless technologies for the Internet of Things

In the next generation of wireless communication networks, a large number of low-power IoT devices or sensors are deployed. So I conducted research on the current wireless communication technology of the Internet of Things and sorted out [30]:

	WiFI	Zigbee	Bluetooth	Cellular(4G, 5G)	LORA
High speed support	/	/	/	YES	/
High Density support	/	/	/	YES	/
Throughput	LOW	LOW	LOW	HIGH	LOW
Low Latency	YES	YES	YES	YES	YES
Range	MEDIUM	LOW	LOW	HIGH	HIGH
Reliability	LOW	LOW	LOW	HIGH	LOW

2.4 WPT System

The WPT system can absorb and utilize energy in the environment, such as heat energy, wind energy, sound energy, and radio frequency energy. Compared to currently existing batteries and charged supercapacitors, the environment provides high-quality energy. The utilization of natural energy sources in energy harvesting procedures inside communication networks has recently been the subject of various research [31, 32]. Energy harvesting from natural sources is not as efficient as anticipated since environmental sources are erratic and unpredictable. The primary energy harvesting approaches also only work in certain situations and are scenario-specific [33]. One EH technology, known as WPT, circumvents the aforementioned drawbacks [34] by allowing communication network nodes to recharge their internal batteries using electromagnetic radiation. In WPT, there are two methods for collecting green energy: one option exploits a base station or another specialized, completely regulated power source. Recent WPT-based contributions have emphasized near-field (short-range) energy transmission rather than far-field (long-range) energy transfer. The application situation affects the distances at the near-field and far-field ends. For instance, the near-field distance of wireless electromagnetic power exchange in both indoor and outdoor situations can only be a few meters, but the far-field distance may be a few kilometers [35]. There are a number of drawbacks to near-field WPT, including distance restrictions, the inability to keep the field strength at safe levels, high initial costs, the adoption of high frequencies for the power supply, and impractical air ionization methods [35]. Another drawback is the difficulty of tuning resonant induction. As a result, more advancements in far-field WPT technology are required. A requirement for technologies that can concurrently send information and power to endpoint devices has arisen from the possibility of combining WPT with communications networks. The concept of SWIPT was initially presented for this need from a theoretical standpoint[34]. Wireless communication networks have recently given SWIPT a lot of attention [36, 37]. SWIPT technology is crucial for the transfer of energy and information in a range of contemporary communication networks in the age of 5G communications.

2.5 SWIPT Systems

SWIPT was initially introduced as a theoretical idea in 8. Actually, a lot of task-processing systems combine the processing of energy and information. Energy, matter, or anything similar must be modulated in order to represent a signal. It's not always necessary to keep communications and media separate. Early examples of such systems include telegraphs, telephones, and crystal radios [38], none of which required an external power source. Harvesting the incoming energy may also be advantageous for contemporary communication systems that must operate within severe energy limits [39]. Mobile device charging may be done efficiently using strong base stations or other specialized nodes [40, 41]. In the backscatter link, the energy of the

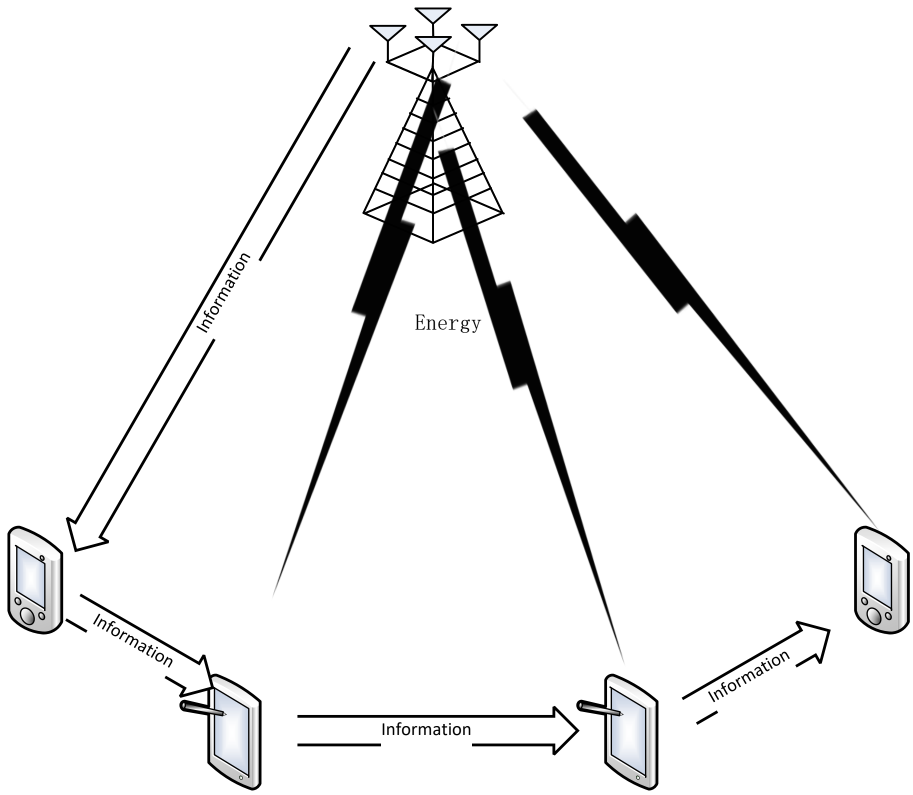

Figure 2.1: SWIPT System.

downlink is exploited to drive the scatter tag to transmit the uplink information [34].

Enable SWIPT is expected to information exchange between wireless devices and wireless energy transfer to communication devices. Harvesting energy from the environment is an efficient approach for wireless communication networks where all devices are powered by batteries, and the radio signal in the environment is an ideal energy harvesting source. In fact, passive gadgets driven by radio signal energy have become widely adopted, such as RFID, backscattering tags, and sensor networks that are intended to be implanted in human bodies [10]. Since the resources of the SWIPT system are limited, the resource allocation algorithm becomes significantly important. [42, 43] mainly focuses on the application of resource allocation algorithms and obtaining the optimal resource allocation strategy. Most passive devices and low-power devices do not have encryption capability, which leads to information security issues in the SWIPT network [44].

2.6 Physical Layer Security

Wireless networks are widely employed in both the military and the civilian worlds and have ingrained themselves into our daily lives. When individuals heavily rely on wireless networks to send sensitive data like credit card transactions or bank-related data transfers, security becomes a crucial concern in wireless applications. Therefore, it is crucial to be able to reliably communicate sensitive information in the presence of enemies. Attackers may try to carry out a number of assaults to obtain unauthorized access to, modify, or even stop the flow of information [45]. The majority of security measures rely on encryption technologies adopted on the wireless network's higher tiers. The public-private key is often shared by two users for symmetric encryption methods like the Data Encryption Standard. For key exchange, if none of the two users has this private key, a secure channel is needed. Here, physical layer techniques may be utilized to distribute keys, offer location privacy, and support upper-layer security algorithms instead of extra channels. Physical layer security techniques make it more challenging for attackers to decode the delivered data. The five kinds of physical layer security approach now in the application include theoretical security capacity, power, coding, channel, and signal-detecting techniques.

Physical layer security is an alternative to cryptographic encryption at the application layer, in fact, exploiting the characteristics of wireless channel fading to achieve completely secure communication is called physical layer security. Completely confidential communication is possible when the eavesdropper's channel is a downgrade version of the target user, according to Wyner's pioneering work [46]. The capacity difference between the target user and the eavesdropper is generally referred to as the secrecy rate [47, 48] :

$$R = \left[\log_2\left(1 + SINR_{users}\right) - \log_2\left(1 + SINR_{eavesdropper}\right)\right]^{\dagger} \tag{2.1}$$

When $R = 0$, it means that the eavesdropper can fully decode the desired information.

2.7 Distributed Antenna CoMP Systems

A Distributed Antenna System is a network that geographically disperses various transmitting and receiving stations and connects each base station to the same central processing unit. In a cellular network, the antennas are usually scattered around the cell. This is sensible because the average distance between the antennas is shorter, which reduces the transmit power required to

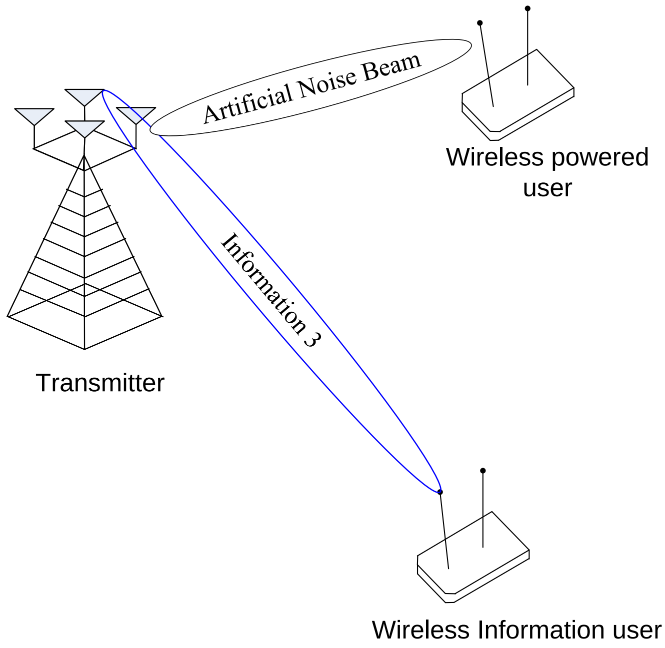

Figure 2.2: Secure SWIPT System by adopting Artificial Noise and Beamforming.

maintain fixed channel quality and improves coverage. [49].

The distributed antenna multi-point coordinated (CoMP) transmission system can expand the service range and improve spectral efficiency to reduce interference. The CoMP network adopts a cloud computing architecture, which separates the communication and information processing functions of traditional base stations, centralizes all the gathered information in the central processor for processing, and the physics distributed remote radio frequency heads so that RRH only undertakes all radio frequencies. operations, such as power amplification and analog filtering, in addition, all RRHs are connected by backhaul links to the central processing unit. The inherent architecture of CoMP systems enables them to provide spatial diversity against path loss and shadow fading[22]. Studies have shown that CoMP systems can provide significant system performance gains when fully cooperative is enabled [50]. However, due to various physical constraints, the backhaul capacity is limited, so CoMP systems with limited backhaul capacity constraints received widespread attention. The backhaul capacity is the maximum information capacity in the backhaul link, and in distributed antenna systems it is the sum of the information capacity of each RRH [22, 19].

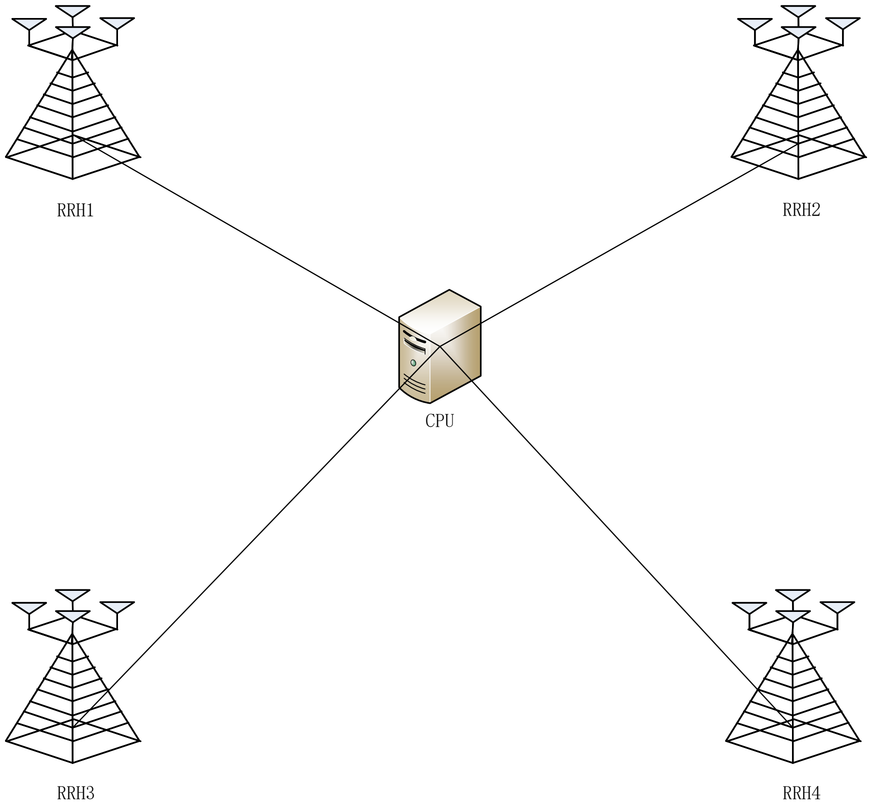

Figure 2.3: Distributed Antenna CoMP System.

2.8 Convex and Non-Convex optimization

Signal processing and wireless communications both benefit greatly from the exploitation of quadratically constrained quadratic programming (QCQPs). In particular, QCQPs are not convex are often NP-hard. Existing techniques, such as employing consecutive convex approximations together with computer iteration provide close to optimum suboptimal solutions. Positive semi-definite relaxations and linear approximations have also been adopted to addressnon-convex problems [51]. There is also some research showing that machine learning can solve some non-convex problems [52]–[59].

We occasionally have to deal with a non-convex situation that has $\mathbf{x}^H\mathbf{C}\mathbf{x} > 0$ or $\mathbf{x}^H\mathbf{C}\mathbf{x} = 0$. Hence, we employ the operators $\mathrm{Tr}(\mathbf{x}^H\mathbf{C}\mathbf{x}) = \mathbf{x}^H C\mathbf{x}$ and $\mathrm{Tr}(\mathbf{x}^H\mathbf{C}\mathbf{x}) = \mathrm{Tr}(\mathbf{x}\mathbf{x}^H\mathbf{C}) = \mathrm{Tr}(\mathbf{X}\mathbf{C})$ to address this problem. We can see that the rank$(\mathbf{X})$ for this approach is 1. After transformation, we discover that the sole non-convex constraint for the issue is rank$(\mathbf{X}) = 1$. If we ignore this circumstance, the whole problem has been reduced to a convex problem that can be resolved by CVX methods, this is why the method is called SDR. Engineering allows us to either disregard this requirement or demonstrate that the question of whether such a condition exists or not is equivalent [60].

The successive convex approximation is a method of linearizing the function by using the Taylor first-order expansion of the function, which can convert some non-convex functions into approximate linear convex functions. This method adopts a linear function that is closer to the original function to approximate through continuous iteration. The iterative process is convergent and monotonic, and from the algorithm point of view, the method has polynomial complexity [61, 62].

Chapter 3

System Description and Problem Formulation

3.1 Network Topology

The CoMP system in this thesis regulates L RRHs to accommodate various sorts of users. The CoMP system employs artificial noise beams to aid energy-harvesting receivers and information beams to assist information consumers. The central processor's aim is to employ artificial noise beam and information beamforming technologies to safeguard information consumers with SINRs greater than the SINR decoding threshold. Furthermore, we use these technologies to establish physical layer security by lowering the SINR of eavesdroppers and energy harvesting receivers, preventing them from decoding the incoming message. At the same time, we observe that this system's backhaul capacity is constrained, it ought to be less than the processor's maximum processing capability. In order to reduce this wireless coordinated multipoint network's power consumption, we imposed four limits.

Constraints:

1. Energy harvesters' SINR has to be less than the decoding threshold.
2. Eavesdroppers' SINR has to be lower than the SNIR of the decoding threshold.
3. Information users' SINR has to be higher than the SNIR of the decoding threshold.
4. The backhaul capacity needs to be less than the threshold for maximum backhaul capacity.

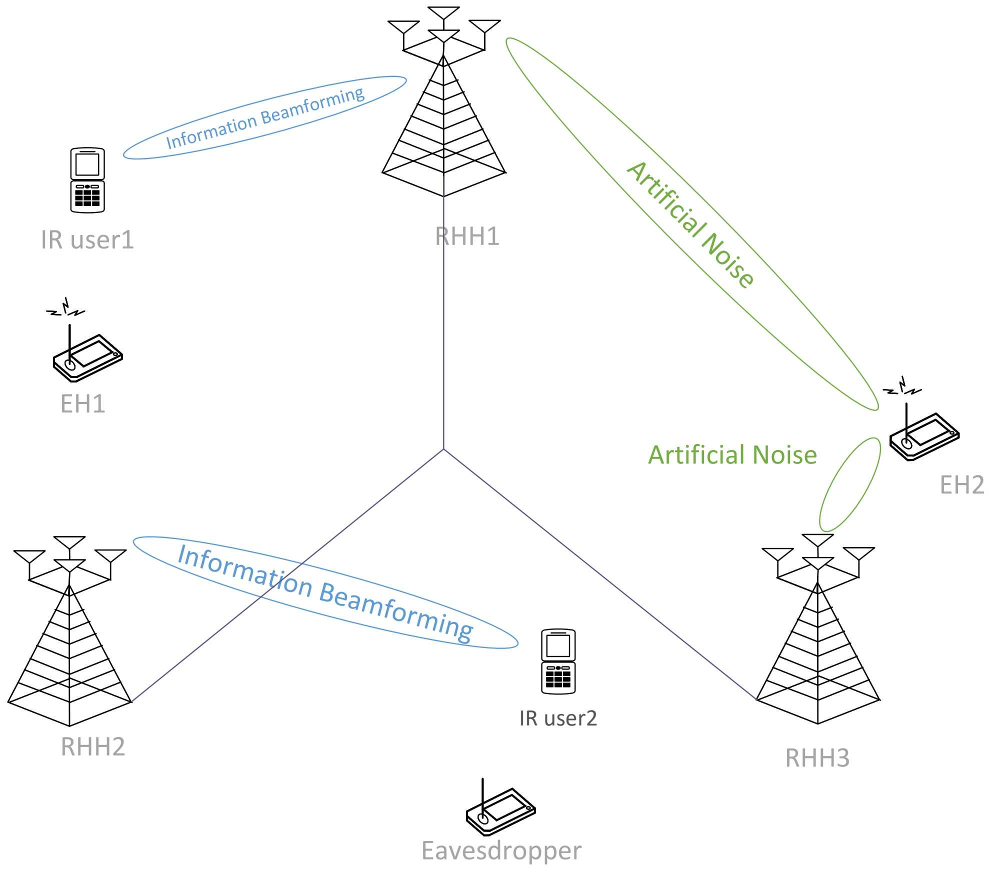

Figure 3.1: System model with L=3 RRHs for illustration.

While the RRH solely handles RF and information transmission tasks, such as signal amplification and transmission, the multi-point coordination network employs the central processing unit to perform base station and signal processing portion operations. To meet the goals of expanding coverage, enhancing anti-interference capability, and minimizing resource consumption, we can pick the resource allocation technique to determine the operating mode of the RRH.

The network in Figure 3.1 has three RRHs that can work together, and there are k information users, m energy users, and n eavesdroppers, each RRH can transmit information beams and artificial noise to achieve the above goals.

3.1.1 Notation:

We use bold capital and lowercase characters to denote matrices and vectors, respectively. Rank($\mathbf{A}$), Tr($\mathbf{A}$), $\mathbf{A}^H$ has been exploited to represent the trace and Hermitian transpose of the matrix $\mathbf{A}$. Positive-definite and a positive semidefinite matrix is defined as $\mathbf{A} \succ \mathbf{0}$ and $\mathbf{A} \succeq \mathbf{0}$, respectively. $\mathbf{I_N}$ is set as the $\mathbf{N} \times \mathbf{N}$ identity matrix. $\mathbf{N^{N \times M}}$ represents all $\mathbf{N} \times \mathbf{M}$ matrices with complex entries.Adopt $\mathbf{N} \times \mathbf{N}$ to express the collection of all Hermitian matrices, .$\|$ A represents a vector's norm.

3.2 Wireless Channel Model

We establish the channel to be a frequency flat fading channel and concentrate on a time-division duplexing scheme. By employing handshaking and channel reciprocity, the RRH may gather channel status data for every receiver. Then, they send the CSI to the Central processor for computation to determine the resource allocation method.

The received signals at IR $k \in \{1,\ldots,K\}$, ER $m \in \{1,\ldots,M\}$ and eav $n \in \{1,\ldots,N\}$ (This means we have K information users, M energy harvesters and N eavesdroppers)are given by:

$$\text{Received signal at IR}: \quad y_k = \sum_{l=1}^{L} \mathbf{h}_k^H \left(a_{l,k}\mathbf{w}_{l,k}s_{l,k} + \mathbf{v}\right) + \sum_{l=1}^{L}\sum_{j\neq k}^{K} \mathbf{h}_k^H \left(a_{l,j}\mathbf{w}_{l,j}s_{l,j} + \mathbf{v}\right) + \sigma_s^2. \tag{3.1}$$

$$\text{Received signal at ER}: \quad y_m = \sum_{l=1}^{L} \mathbf{g}_m^H \left(a_{l,m}\mathbf{w}_{l,m}s_{l,m} + \mathbf{v}\right) + \sum_{l=1}^{L}\sum_{j\neq m}^{M} \mathbf{g}_m^H \left(a_{l,j}\mathbf{w}_{l,j}s_{l,j} + \mathbf{v}\right) + \sigma_s^2. \tag{3.2}$$

$$\text{Received signal at Eve}: \quad y_n = \sum_{l=1}^{L} \mathbf{q}_n^H \left(a_{l,n}\mathbf{w}_{l,n}s_{l,n} + \mathbf{v}\right) + \sum_{l=1}^{L}\sum_{j\neq n}^{N} \mathbf{q}_n^H \left(a_{l,j}\mathbf{w}_{l,j}s_{l,j} + \mathbf{v}\right) + \sigma_s^2. \tag{3.3}$$

The $\mathbf{h}$, $\mathbf{g}$, and $\mathbf{q}$in the period are all fading rician channels which are defined as:

$$\mathbf{h}_k = \sqrt{\frac{K}{K+1}}\mathbf{h}_d + \sqrt{\frac{1}{K+1}}\mathbf{h}_s, \tag{3.4}$$

$$\mathbf{g}_m = \sqrt{\frac{K}{K+1}}\mathbf{g}_d + \sqrt{\frac{1}{K+1}}\mathbf{g}_s, \tag{3.5}$$

$$\mathbf{q}_n = \sqrt{\frac{K}{K+1}}\mathbf{q}_d + \sqrt{\frac{1}{K+1}}\mathbf{q}_s, \tag{3.6}$$

where $\mathbf{h}_d$, $\mathbf{g}_d$, $\mathbf{q}_d$ represents a unit-amplitude deterministic complex scalar that contains the LoS and specular components of the channel, and $\mathbf{h}_s$, $\mathbf{g}_s$, $\mathbf{q}_s$ represents that the scattering component of the channel is a zero-mean-unit-variance circular symmetric complex Gaussian random.

$a_{l,k}$ is the RRH scheduling indicator, which is a binary variable and can only be 0 or 1. 1 means that the RRH serves the user normally, and 0 means that the RRH does not provide services. $\mathbf{w}_k \in \mathbb{C}^{N_t \times 1}$ is the beamforming vector for the low k users' beamforming vector. $\mathbf{v}$ is the beamforming vector for the artificial noise beamforming vector. $A_{l,k} = \operatorname{diag}\left(a_{l,k}, \ldots, a_{l,k}\right) \in \mathbb{B}^{N_t \times N_t}$. $A_k = \operatorname{diag}\left(A_{1,k}, \ldots, A_{L,k}\right)$

In the distributed antenna system, the SNIR of IF, ER, eva is defined as:

$$\text{SINR of IR:} \quad \Gamma_k = \frac{\left|\mathbf{h}_k^H \mathbf{A}_k \mathbf{w}_k\right|^2}{\sum_{j \neq k}^K \left|\mathbf{h}_k^H \mathbf{A}_j \mathbf{w}_j\right|^2 + Tr\left(\mathbf{h}_k \mathbf{h}_k^H \mathbf{V}\right) + \sigma_s^2} \tag{3.7}$$

$$\text{SINR of ER:} \quad \Gamma_m = \frac{\eta \left|\mathbf{g}_m^H \mathbf{A}_k \mathbf{w}_k\right|^2}{\sum_{j \neq k}^K \left|\mathbf{g}_m^H \mathbf{A}_j \mathbf{w}_j\right|^2 + Tr\left(\mathbf{g}_m \mathbf{g}_m^H \mathbf{V}\right) + \sigma_s^2} \tag{3.8}$$

$$\text{SINR of Eve:} \quad \Gamma_n = \frac{\left|\mathbf{q}_n^H \mathbf{A}_k \mathbf{w}_k\right|^2}{\sum_{j \neq k}^K \left|\mathbf{q}_n^H \mathbf{A}_j \mathbf{w}_j\right|^2 + Tr\left(\mathbf{q}_n \mathbf{q}_n^H \mathbf{V}\right) + \sigma_s^2} \tag{3.9}$$

where Γ is the received signal-to-interference-plus-noise ratio at the desired receiver.

3.3 Problem Formulation

To obtain the optimal solution that minimizes the transmit power, the answer can be obtained by solving problem (P1), where $\mathbf{w}_k, \mathbf{w}_{l,k}, a_{l,k}, \mathbf{V}$ are the variables.

$$(P1) \quad : \quad \underset{\left\{\mathbf{A}_k, \mathbf{w}_k, \mathbf{w}_{l,k}, a_{l,k}, \mathbf{V}\right\}}{\text{minimize}} \quad \left\|\mathbf{A}_k \mathbf{w}_k\right\|^2 + \operatorname{Tr}\left(\mathbf{V}\right), \tag{3.10}$$

$$s.t. \quad \text{C1}: \quad a_{l,k}[n] \in \{0,1\}, \forall n, k, \tag{3.11}$$

$$\text{C2}: \quad \Gamma_k \geq \gamma_k \quad \forall k, \tag{3.12}$$

$$\text{C3}: \quad \sum_{k=1}^K a_{l,k} \log_2\left(1 + \Gamma_k\right) \leq C_l, \quad \forall l, \tag{3.13}$$

$$\text{C4}: \quad \Gamma_m < \Gamma_{th}, \quad \forall m \tag{3.14}$$

$$\text{C5}: \quad \Gamma_n < \Gamma_{th}, \quad \forall n \tag{3.15}$$

$$\text{C6}: \quad \sum_{k=1}^K a_{l,k} \left\|\mathbf{w}_{l,k}\right\|^2 \leq P_{\max}, \quad \forall l. \tag{3.16}$$

C1 is a binary constraint on the RRH scheduling indicator. The variable γ_k in C2 specifies the minimum required SINR of the receiver required to decode the information. C3 is the constraint on the backhaul capacity per RRH, where C_l is the maximum backhaul capacity per base station. C4 and C5 represent the SNIR of the ER and the SNIR of the eavesdropper, respectively, which are both less than the decoding threshold. The maximum transmission power limit for each RRH is defined as C6.

Chapter 4

Design solution to Distributed Antenna Systems

4.1 Problem Analysis and Summary

It is possible to categorize the optimization problem in (3.10) as a non-convex quadratic restricted quadratic programming problem (QCQP) [51]. The non-convexity is due to the quadratic coupling to the information-carrying beamforming vector $\mathbf{w}_k$, and the RRH scheduling indicator $a_{l,k}$ is a discrete binary integer. The coupling of $a_{l,k}$ and the function with respect to $\mathbf{w}_k$ also leads to some conditions being nonconvex.C1, C2, C3, C6 are all non-convex conditions. Nonconvex optimisation problems are typically difficult to solve and have no set solution method. As a result, we reformat the problem as a convex optimization problem using the positive semi-definite relaxation of semi-definite programming [60].

4.2 Semidefinite Programming Relaxation

For facilitating the SDP relaxation, In order to facilitate the formulation of the formula, we introduce $\mathbf{H}_k = \mathbf{h}_k\mathbf{h}_k^H$, $\mathbf{G}_m = \mathbf{g}_m\mathbf{g}_m^H$, $\mathbf{Q}_n = \mathbf{q}_n\mathbf{q}_n^H$, we define $\mathbf{W}_k = \mathbf{w}_k\mathbf{w}_k^H$,$\mathbf{W}_{l,k} = \mathbf{w}_{l,k}\mathbf{w}_{l,k}^H$ and rewrite problem (3.10) in terms of $\mathbf{W}$ as:

$$
\begin{aligned}
(P2) \quad : \quad & \underset{\{\mathbf{A}_k,\mathbf{w}_k,\mathbf{w}_{l,k},a_{l,k},\mathbf{V}\}}{\text{minimize}} \quad \mathrm{Tr}\left(\mathbf{A}_k\mathbf{A}_k^H\mathbf{W}_k\right)+\mathrm{Tr}\left(\mathbf{V}\right), && (4.1)\\
s.t. \quad \mathrm{C1}: \quad & a_{l,k}[n]\in\{0,1\}, \forall n,k, && (4.2)\\
\mathrm{C2}: \quad & \frac{\mathrm{Tr}\left(\mathbf{A}_k\mathbf{A}_k^H\mathbf{H}_k\mathbf{W}_k\right)}{\gamma_k} \geq \textstyle\sum_{j\neq k}^{k}\mathrm{Tr}\left(\mathbf{A}_j\mathbf{A}_j^H\mathbf{H}_k\mathbf{W}_j\right)+\mathrm{Tr}\left(\mathbf{H}_k\mathbf{V}\right)+\sigma_s^2, \quad \forall k, && (4.3)\\
\mathrm{C3}: \quad & \sum_{k=1}^{K} a_{l,k}\log_2\left(1+\Gamma_k\right)\leq C_l, \quad \forall l, && (4.4)\\
\mathrm{C4}: \quad & \frac{\eta\mathrm{Tr}\left(\mathbf{A}_k\mathbf{A}_k^H\mathbf{G}_m\mathbf{W}_k\right)}{\Gamma_{th}} < \textstyle\sum_{j\neq k}^{k}\mathrm{Tr}\left(\mathbf{A}_j\mathbf{A}_j^H\mathbf{G}_m\mathbf{W}_j\right)+\mathrm{Tr}\left(\mathbf{G}_m\mathbf{V}\right)+\sigma_s^2, \quad \forall m, && (4.5)\\
\mathrm{C5}: \quad & \frac{\mathrm{Tr}\left(\mathbf{A}_k\mathbf{A}_k^H\mathbf{Q}_n\mathbf{W}_k\right)}{\Gamma_{th}} < \textstyle\sum_{j\neq k}^{k}\mathrm{Tr}\left(\mathbf{A}_j\mathbf{A}_j^H\mathbf{Q}_n\mathbf{W}_j\right)+\mathrm{Tr}\left(\mathbf{Q}_n\mathbf{V}\right)+\sigma_s^2, \quad \forall n, && (4.6)\\
\mathrm{C6}: \quad & \sum_{k=1}^{K} a_{l,k}\mathrm{Tr}\left(\mathbf{W}_{l,k}\right)\leq P_{\max}, \quad \forall l. && (4.7)
\end{aligned}
$$

The main challenge of this problem is the non-convexity introduced by the coupling of the $\mathbf{A}_k\mathbf{A}_k^H$ and $\mathbf{W}_k$. In order to solve the coupling problem of various $\mathbf{A}_k$, $\mathbf{w}_k$, $\mathbf{w}_{l,k}$ $\mathbf{W}_k$ matrices, we regard $\mathbf{A}_k\mathbf{w}_k$ as a whole. we set $\bar{\mathbf{W}}_{l,k}=a_{l,k}\mathbf{W}_{l,k}$ and $\mathbf{W}_{l,k}=\mathbf{w}_{l,k}\mathbf{w}_{l,k}^H$. To solve the non-convex problem of C6, the Big m method is adopted [63].

$$(P3) \quad : \underset{\{\mathbf{A}_k,\mathbf{w}_k,\mathbf{w}_{l,k},a_{l,k},\mathbf{V}\}}{\text{minimize}} \quad \text{Tr}\left(\bar{\mathbf{W}}_k\right)+\text{Tr}\left(\mathbf{V}\right), \tag{4.8}$$

$$s.t. \quad \text{C1}: \quad a_{l,k}\in\{0,1\}, \forall n,k, \tag{4.9}$$

$$\text{C2}: \quad \frac{\text{Tr}\left(\mathbf{H}_k\bar{\mathbf{W}}_k\right)}{\gamma_k} \geq \textstyle\sum_{j\neq k}^{k}\text{Tr}\left(\mathbf{H}_k\bar{\mathbf{W}}_j\right)+\text{Tr}\left(\mathbf{H}_k\mathbf{V}\right)+\sigma_s^2, \quad \forall k, \tag{4.10}$$

$$\text{C3}: \quad \sum_{k=1}^{K} a_{l,k}\log_2\left(1+\Gamma_k\right)\leq C_l, \quad \forall l, \tag{4.11}$$

$$\text{C4}: \quad \frac{\eta\text{Tr}\left(\mathbf{G}_m\bar{\mathbf{W}}_k\right)}{\Gamma_{th}} < \textstyle\sum_{j\neq k}^{k}\text{Tr}\left(\mathbf{G}_m\bar{\mathbf{W}}_j\right)+\text{Tr}\left(\mathbf{G}_m\mathbf{V}\right)+\sigma_s^2, \quad \forall m, \tag{4.12}$$

$$\text{C5}: \quad \frac{\text{Tr}\left(\mathbf{Q}_n\bar{\mathbf{W}}_k\right)}{\Gamma_{th}} < \textstyle\sum_{j\neq k}^{k}\text{Tr}\left(\mathbf{Q}_n\bar{\mathbf{W}}_k\right)+\text{Tr}\left(\mathbf{Q}_n\mathbf{V}\right)+\sigma_s^2, \quad \forall n, \tag{4.13}$$

$$\text{C6}: \quad \sum_{k=1}^{K}\text{Tr}\left(\bar{\mathbf{W}}_{l,k}\right)\leq P_{\max}, \quad \forall l, \tag{4.14}$$

$$\text{C7}: \quad \bar{\mathbf{W}}_{l,k}\preceq P_{\max}\mathbf{I}_{N_t}a_{l,k}, \quad \forall l,k, \tag{4.15}$$

$$\text{C8}: \quad \bar{\mathbf{W}}_{l,k}\preceq \mathbf{W}_{l,k}, \quad \forall l,k, \tag{4.16}$$

$$\text{C9}: \quad \bar{\mathbf{W}}_{l,k}\succeq \mathbf{W}_{l,k}-\left(1-a_{l,k}\right)P_{\max}\mathbf{I}_{N_t}, \quad \forall l,k, \tag{4.17}$$

$$\text{C10}: \quad \text{Rank}\left(\bar{\mathbf{W}}_{l,k}\right)=1, \quad \forall l,k, \tag{4.18}$$

$$\text{C11}: \quad \bar{\mathbf{W}}_{l,k}\succeq \mathbf{0}, \quad \forall l,k. \tag{4.19}$$

$$\tag{4.20}$$

It can be noticed that the matrix coupling of C2, C3, C4, C5, and C6 has been resolved. C10, C11 are adopted to guarantee $\bar{\mathbf{W}}_{l,k}=a_{l,k}\mathbf{W}_{l,k}$ and $\mathbf{W}_{l,k}=\mathbf{w}_{l,k}\mathbf{w}_{l,k}^H$. In this way, $\mathbf{A}_k$ and $\mathbf{w}_k$ can be decoupled, where $\bar{\mathbf{W}}_k=\bar{\mathbf{w}}_k\bar{\mathbf{w}}_k^H$ and $\bar{\mathbf{w}}_k=\mathbf{A}_k\mathbf{w}_k$. And the signal-to-noise ratio of IF can be re-expressed as:

$$\text{SINR of IR:} \quad \bar{\Gamma}_k=\frac{\text{Tr}\left(\mathbf{H}_k\bar{\mathbf{W}}_k\right)}{\sum_{j\neq k}^{K}\text{Tr}\left(\mathbf{H}_k\bar{\mathbf{W}}_j\right)+Tr\left(\mathbf{h}_k\mathbf{h}_k^H\mathbf{V}\right)+\sigma_s^2}. \tag{4.21}$$

C1 is obviously a non-convex constraint, because this is a binary discrete integer value, we can relax this constraint and rewrite it as:

$$\text{C1a}: \quad \sum_{n=1}^{N}\sum_{k=1}^{K}a_{l,k}-a_{l,k}^2\leq 0, \forall n,k, \tag{4.22}$$

$$\text{C1b}: \quad 0\leq a_{l,k}\leq 1, \quad \forall n,k, \tag{4.23}$$

Unfortunately, C1a is still a non-convex condition, so the first-order Taylor expansion of this condition is adopted to rewrite the condition as:

$$\mathrm{C1a}^{'}: \quad \sum_{n=1}^{N}\sum_{k=1}^{K} a_{l,k} - \sum_{n=1}^{N}\sum_{k=1}^{K} a_{l,k}^{(t)} a_{l,k} - \left(a_{l,k}^{(t)}\right)^2 \leq 0, \forall n, k, \tag{4.24}$$

$$\tag{4.25}$$

Since we decouple the matrix, C3 can be rewritten as:

$$\mathrm{C3}^{'}: \quad \sum_{k=1}^{K} log_2(\varphi_k) - \sum_{k=1}^{K} log_2(\delta_k) \leq C_l, \quad \forall k, \tag{4.26}$$

$$\mathrm{C12}: \quad \varphi_k \geq \sum_{k=1}^{K} \mathrm{Tr}\left(\mathbf{H}_k \bar{\mathbf{W}}_k\right) + \mathrm{Tr}\left(\mathbf{H}_k \mathbf{V}\right) + \sigma_s^2 \quad \forall k, \tag{4.27}$$

$$\mathrm{C13}: \quad \delta_k \leq \sum_{j \neq k}^{K} \mathrm{Tr}\left(\mathbf{H}_k \bar{\mathbf{W}}_j\right) + \mathrm{Tr}\left(\mathbf{H}_k \mathbf{V}\right) + \sigma_s^2 \quad \forall k, \tag{4.28}$$

Since the log function in C3' is a concave function, the entire C3 is a non-convex limit, so we perform Taylor first-order expansion on it:

$$\mathrm{C3}^{''}: \quad \sum_{k=1}^{K} \left(log_2(\varphi_k^{(t)}) + \frac{\varphi_k - \varphi_k^{(t)}}{\varphi_k^{(t)} \ln 2} \right) - \sum_{k=1}^{K} log_2(\delta_k) \leq C_l, \quad \forall k, \tag{4.29}$$

In order to circumvent the non-convexity brought by C10, this constraint will be relaxed using SDR. The following theorem proves the tightness of SDR.

*Theorem*1. For $P_{max} > 0$, an optimal beamforming rank-one matrix $\bar{\mathbf{W}}_{l,k}^{\star}$ can always be obtained.

Proof: Please refer to Appendix 1.

The whole optimization problem can be written as :

$$(P4) \quad : \underset{\{\mathbf{A}_k,\mathbf{w}_k,\mathbf{w}_{l,k},a_{l,k},\mathbf{V}\}}{\text{minimize}} \quad \text{Tr}\left(\bar{\mathbf{W}}_k\right)+\text{Tr}\left(\mathbf{V}\right), \tag{4.30}$$

$$s.t. \quad \text{C1a}^{'}: \quad \sum_{n=1}^{N}\sum_{k=1}^{K} a_{l,k}-\sum_{n=1}^{N}\sum_{k=1}^{K} a_{l,k}^{(t)}a_{l,k}-\left(a_{l,k}^{(t)}\right)^2 \leq 0,\forall n,k, \tag{4.31}$$

$$\text{C1b}: \quad 0\leq a_{l,k}\leq 1, \quad \forall n,k, \tag{4.32}$$

$$\text{C2}: \quad \frac{\text{Tr}\left(\mathbf{H}_k\bar{\mathbf{W}}_k\right)}{\gamma_k} \geq \sum_{j\neq k}^{k}\text{Tr}\left(\mathbf{H}_k\bar{\mathbf{W}}_j\right)+\text{Tr}\left(\mathbf{H}_k\mathbf{V}\right)+\sigma_s^2, \quad \forall k, \tag{4.33}$$

$$\text{C3}^{''}: \quad \sum_{k=1}^{K}\left(log_2(\varphi_k^{(t)})+\frac{\varphi_k-\varphi_k^{(t)}}{\varphi_k^{(t)}\ln 2}\right)-\sum_{k=1}^{K}log_2(\delta_k)\leq C_l, \quad \forall k, \tag{4.34}$$

$$\text{C4}: \quad \frac{\eta\text{Tr}\left(\mathbf{G}_m\bar{\mathbf{W}}_k\right)}{\Gamma_{th}} < \sum_{j\neq k}^{k}\text{Tr}\left(\mathbf{G}_m\bar{\mathbf{W}}_j\right)+\text{Tr}\left(\mathbf{G}_m\mathbf{V}\right)+\sigma_s^2, \quad \forall m, \tag{4.35}$$

$$\text{C5}: \quad \frac{\text{Tr}\left(\mathbf{Q}_n\bar{\mathbf{W}}_k\right)}{\Gamma_{th}} < \sum_{j\neq k}^{k}\text{Tr}\left(\mathbf{Q}_n\bar{\mathbf{W}}_k\right)+\text{Tr}\left(\mathbf{Q}_n\mathbf{V}\right)+\sigma_s^2, \quad \forall n, \tag{4.36}$$

$$\text{C6}: \quad \sum_{k=1}^{K}\text{Tr}\left(\bar{\mathbf{W}}_{l,k}\right)\leq P_{\max}, \quad \forall l, \tag{4.37}$$

$$\text{C7}: \quad \bar{\mathbf{W}}_{l,k}\preceq P_{\max}\mathbf{I}_{N_t}a_{l,k}, \quad \forall l,k, \tag{4.38}$$

$$\text{C8}: \quad \bar{\mathbf{W}}_{l,k}\preceq \mathbf{W}_{l,k}, \quad \forall l,k, \tag{4.39}$$

$$\text{C9}: \quad \bar{\mathbf{W}}_{l,k}\succeq \mathbf{W}_{l,k}-\left(1-a_{l,k}\right)P_{\max}\mathbf{I}_{N_t}, \quad \forall l,k, \tag{4.40}$$

$$\text{C10}: \quad \cancel{\text{Rank}\left(\bar{\mathbf{W}}_{l,k}\right)=1,} \quad \forall l,k \tag{4.41}$$

$$\text{C11}: \quad \bar{\mathbf{W}}_{l,k}\succeq 0, \quad \forall l,k, \tag{4.42}$$

$$\text{C12}: \quad \varphi_k\geq \sum_{k=1}^{K}\text{Tr}\left(\mathbf{H}_k\bar{\mathbf{W}}_k\right)+\text{Tr}\left(\mathbf{H}_k\mathbf{V}\right)+\sigma_s^2 \quad \forall k, \tag{4.43}$$

$$\text{C13}: \quad \delta_k\leq \sum_{j\neq k}^{K}\text{Tr}\left(\mathbf{H}_k\bar{\mathbf{W}}_j\right)+\text{Tr}\left(\mathbf{H}_k\mathbf{V}\right)+\sigma_s^2 \quad \forall k. \tag{4.44}$$

$$\tag{4.45}$$

We can notice that the expression after Taylor expansion will be smaller than the original expression, which makes the solution of P4 must be the solution of P3. P4 is a convex optimization problem that can be solved using the SCA iterative algorithm with polynomial complexity.

Algorithm 1 Successive Convex Approximation Algorithm

1: Initialize parameters $\mathbf{W}_k^{(0)}$, $\mathbf{V}^{(0)}$, $a_{l,k}^{(0)}$, $\varphi_k^{(0)}$,$\delta_k^{(0)}$ set the iteration index $t = 0$, and set the threshold for algorithm latitude $0 < \varepsilon \ll 1$.

2: **while** $\mathrm{Tr}\left(\bar{\mathbf{W}}_k^{(t)}\right) + \mathrm{Tr}\left(\mathbf{V}^{(t)}\right) - \mathrm{Tr}\left(\bar{\mathbf{W}}_k^{(t-1)}\right) - \mathrm{Tr}\left(\mathbf{V}^{(t-1)}\right) \geq \varepsilon$ **do**

3: Obtain $\mathbf{W}_k^{(t)}$, $\mathbf{V}^{(t)}$, $a_{l,k}^{(t)}$, $\varphi_k^{(t)}$,$\delta_k^{(t)}$ by using known $\mathbf{W}_k^{(t-1)}$, $\mathbf{V}^{(t-1)}$, $a_{l,k}^{(t-1)}$, $\varphi_k^{(t-1)}$,$\delta_k^{(t-1)}$ to solving problem $P4$;

4: Update $t \leftarrow t+1$;

5: **end while**

6: **return** $\mathbf{W}_k^{(*)} \leftarrow \mathbf{W}_k^{(t)}$, $\mathbf{V}^{(*)} \leftarrow \mathbf{V}^{(t)}$, $a_{l,k}^{(*)} \leftarrow a_{l,k}^{(t)}$, $\varphi_k^{(*)} \leftarrow \varphi_k^{(t)}$ and $\delta_k^{(*)} \leftarrow \delta_k^{(t)}$.

Note that the rank-one constraint C11 is the source of the remaining nonconvexity in P4. By omitting constraint C11, we employ semidefinite relaxation (SDR) to get around this problem. In general, convex optimization solvers like CVX can effectively address rank constraint relaxation problems. It is understood, nonetheless, that adopting SDR on P4 might not provide a rank-one matrix. We demonstrate the tightness of the adopted SDR in the subsequent theorem.

Problem P4 is solved by the SCA iterative algorithm with polynomial complexity proposed by us, and the local optimal solution of the problem can be obtained. After our simulation, the algorithm has excellent convergence, and it will converge after about 6 or 7 iterations.

Chapter 5

Simulation

This chapter adopts MatLab simulation and illustrates the advantages of the purposed distributed antenna cooperation systems in reducing power consumption.

The following are the parameters used for the simulation:

Parameter	Physical meaning	Value
K	The number of IF users	2
M	The number of EH users	2
N	The number of Eavesdroppers	3
d_r	Reference distance	$10m$
NT	The number of antennas	$6,9,12$
γ_k	Target SNIR desired user	$3,6,9,12,15,18,21$ dB
B	Bandwidth	200 kHz
P_{Iloss}	The path loss coefficient of IR	3.6
P_{Eloss}	The path loss coefficient of EH	2
$P_{eavloss}$	The path loss coefficient of Eavesdroppers	3.6
R_f	Rician factor	6 dB
F_c	Carrier frequency	1.9 GHz
G_t	TX antenna gain	10
G_r	RX antenna gain	3

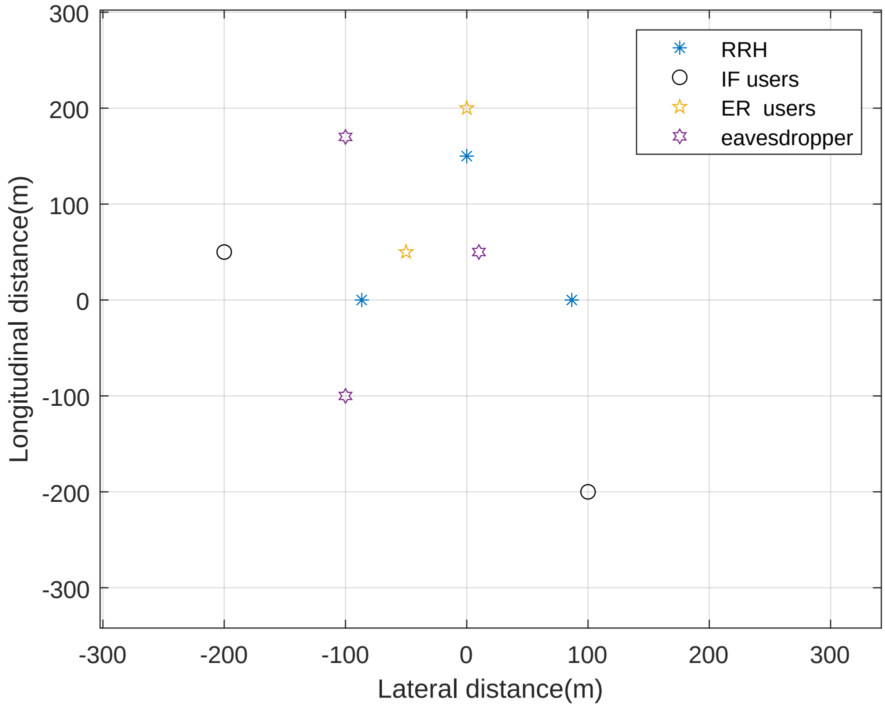

Figure 5.1: Users distribution.

5.1 Results

Figure 5.1 shows the relative positions of RRH, IF users, ER users, and eavesdroppers, and presents them in coordinates. The coordinates of the three RRHs are $\{(-50\sqrt{3},0),(50\sqrt{3},0),(0,150)\}$. The coordinates of IF users and EH users are $\{(-200,50),(100,-200)\}$ and $\{(0,200),(-50,50)\}$ respectively. The coordinates of the eavesdropper are denoted as $\{(10,150),(-100,170),(100,-100)\}$.

Figure 5.2 represents the comparison of energy consumption between multi-point coordinated communication and traditional single-base station communication with different numbers of antennas. In this case, we do not consider the limitation of backhaul capacity and the limitation of power consumption of a single RRH. The abscissa x represents the SINR and the ordinate y represents the total energy consumption. The energy cost of the CoMP system is always lower than that of the traditional single base station antenna with the same antenna. This illustrates that CoMP is more energy efficient than a single base station service when also considering beamforming, eavesdroppers. In the same system, more antennas can significantly

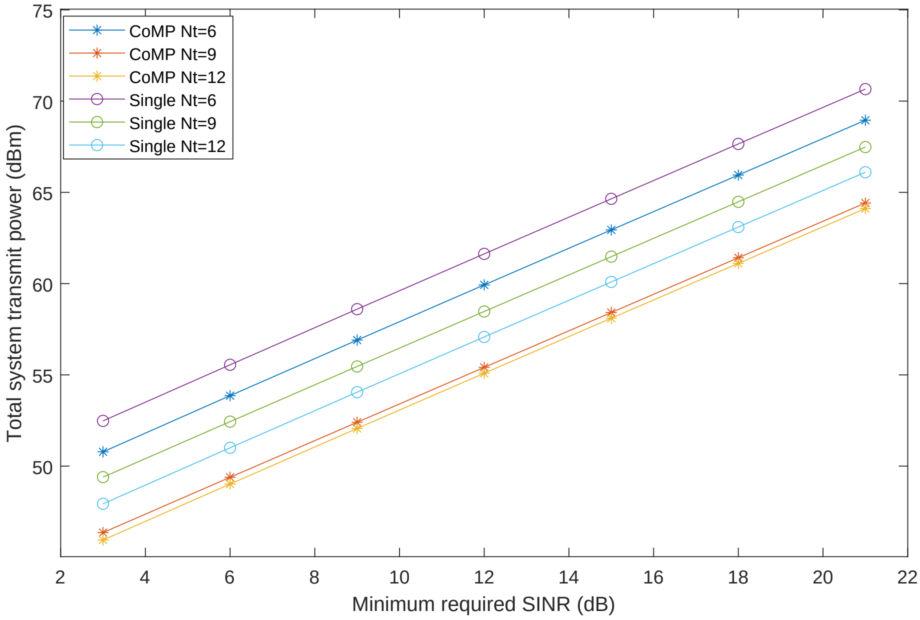

f

Figure 5.2: The performance of CoMP system compared with single base station.

reduce power consumption due to higher spatial degrees of freedom. In addition, the image's general trajectory is upward as the minimum necessary SINR rises. However, this trend will gradually decrease as the power consumption limit is relaxed and finally equals no power consumption limit.

Figure 5.3 shows that in the case of different antennas if the power of a single RRH of the CoMP system is limited, the total power consumption will increase. The abscissa in the figure represents the power consumption limit of a single RRH, and the ordinate represents the system's total energy consumption. Note that although the energy costs of the system is greater than the optimal value when a single RRH is limited, it is still smaller than the energy costs of a single base station. When the transmit power of a single RRH is limited. The transmit power of a certain RRH is already the highest, hence this is the primary cause of the rise in power, but it cannot fully support its users, and other RRHs need to be compensated, thus increasing the power consumption of the entire system.

Figure 5.4 shows that the limited backhaul capacity will prevent the CoMP system from fully cooperating, resulting in higher power consumption than the fully cooperating state, but still lower than that of a single base station. The abscissa x of the figure represents the backhaul capacity, and the ordinate y represents the total energy cost. The general trend is that as the backhaul capacity increases, the system changes from a partially cooperative to a fully cooperative state. Power consumption converges to the lower bound which means no backhaul

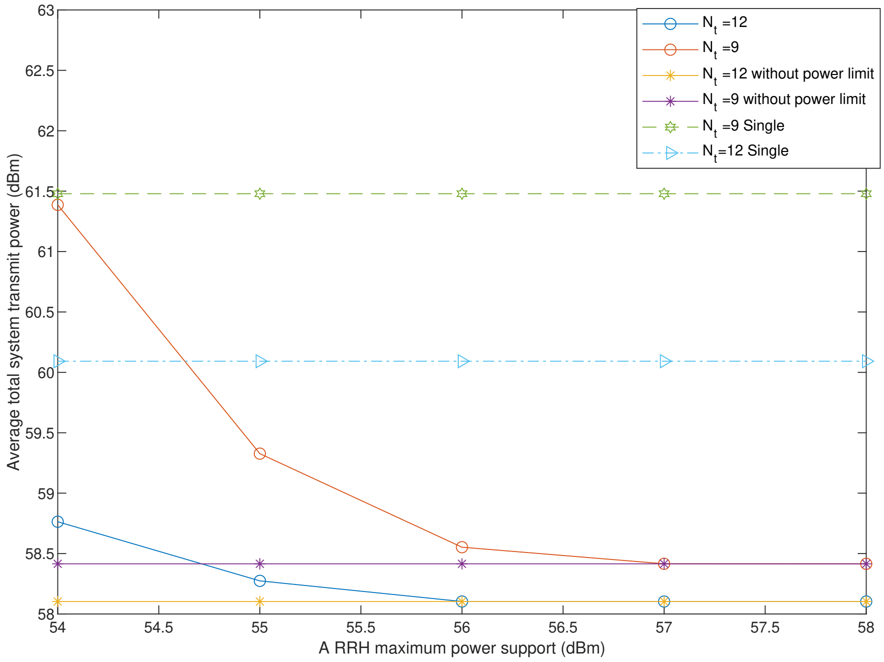

Figure 5.3: The relationship between the maximum energy support of a single RRH and the total energy consumption (in SNIR=15dB, $C_l = \infty$).

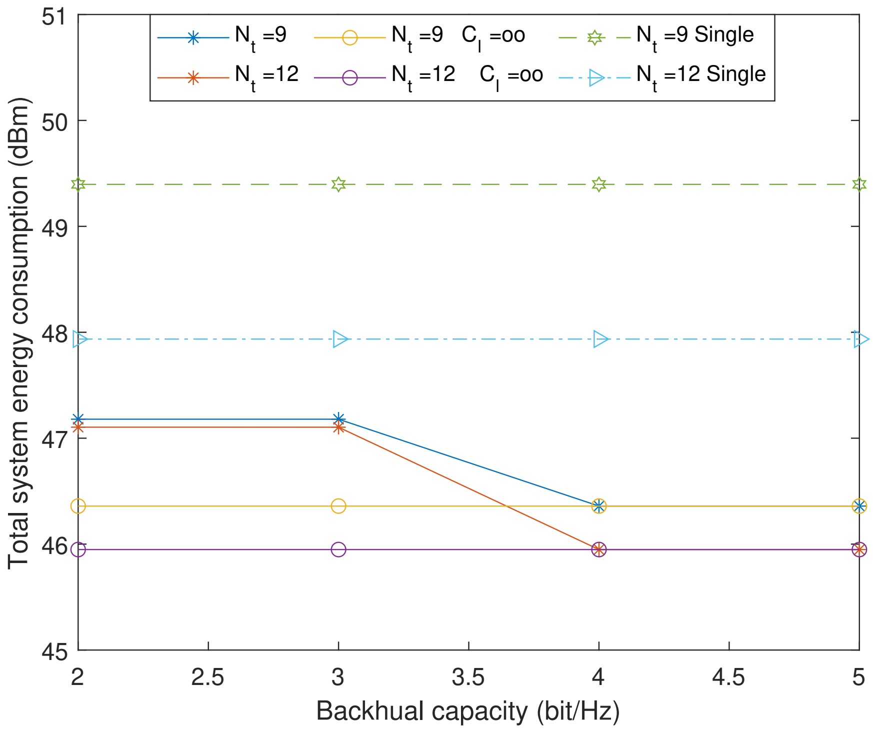

Figure 5.4: Limited Backhaul Capacity (require SINR=3 dB $C_l = 2$ bit/Hz).

capacity limitation. Compared with complete cooperation, incomplete cooperation essentially reduces the degree of spatial freedom, and the anti-fading ability of the system is weakened, causing system power consumption to increase.

5.2 Discussion

The simulation results fully demonstrate the advantages of the distributed antenna multi-point coordination system in terms of energy saving, and the backhaul capacity and the maximum power limit of a single RRH will become the limitations of the system. Even with these limitations, its performance is overall better than a single base station system. However, the adoption of the distributed antenna CoMP system increases the complexity, operation cost, and maintenance cost of the system. Therefore, a trade-off between system complexity and system performance needs to be considered.

Chapter 6

Conclusion

In this thesis, an SCA algorithm with polynomial complexity is proposed to solve the problem iteratively. In addition, we also verified that this algorithm has fast convergence characteristics. Our work verifies the advantages of distributed antenna multi-point coordination systems in terms of energy saving and information security, its essence is to exploit spatial freedom to combat fading and shadows. In addition, the case of limited backhaul capacity and single RRH transmit power is also considered. Artificial noise reduces decoding capabilities for potential eavesdroppers and beamforming improves system energy efficiency. When adopting artificial noise, it needs to trade off the power consumption and the improvement of the security rate, while the distributed antenna CoMP system needs to trade off the system complexity and system performance.

6.1 Future Work

Although our proposed distributed antenna CoMP system has excellent performance, it can be expanded in the future. For example, the RRH is mounted on the UAV, and the dynamic distributed antenna CoMP system can be realized according to the specific terrain and user distribution. Unmanned aerial vehicles (UAVs) are widely used to assist wireless communications because of their flexibility [64, 65, 66, 67, 68]. Hybrid combined CoMP systems of UAVs and fixed base stations will also be considered. There are various studies showing the advantages and prospects of intelligent reflecting surfaces [69, 70, 71, 57], its robust, passive, green, and energy-saving features make it will be widely adopted in the future [72, 73]. The combination of distributed antenna CoMP system and intelligent reflecting surfaces (IRS) is also valuable.

In addition, the complexity of the system, energy efficiency, confidentiality rate, and maximum throughput can also become the direction of future optimization.

Bibliography

[1] A. M. Aris and B. Shabani, "Sustainable power supply solutions for off-grid base stations," *Energies*, vol. 8, no. 10, pp. 10 904–10 941, 2015. [Online]. Available: https://www.mdpi.com/1996-1073/8/10/10904

[2] D. Feng, C. Jiang, G. Lim, L. J. Cimini, G. Feng, and G. Y. Li, "A survey of energy-efficient wireless communications," *IEEE Communications Surveys Tutorials*, vol. 15, no. 1, pp. 167–178, 2013.

[3] E. Oh, B. Krishnamachari, X. Liu, and Z. Niu, "Toward dynamic energy-efficient operation of cellular network infrastructure," *IEEE Communications Magazine*, vol. 49, no. 6, pp. 56–61, 2011.

[4] J. Wu, Y. Zhang, M. Zukerman, and E. K.-N. Yung, "Energy-efficient base-stations sleep-mode techniques in green cellular networks: A survey," *IEEE Communications Surveys & Tutorials*, vol. 17, pp. 803–826, 2015.

[5] Z. Hasan, H. Boostanimehr, and V. K. Bhargava, "Green cellular networks: A survey, some research issues and challenges," *IEEE Communications Surveys Tutorials*, vol. 13, no. 4, pp. 524–540, 2011.

[6] R. S. Prabhu and B. Daneshrad, "Energy-efficient power loading for a mimo-svd system and its performance in flat fading," in *2010 IEEE global telecommunications conference GLOBECOM 2010*. IEEE, 2010, pp. 1–5.

[7] D. W. K. Ng, E. S. Lo, and R. Schober, "Energy-efficient resource allocation in ofdma systems with hybrid energy harvesting base station," *IEEE Transactions on Wireless Communications*, vol. 12, no. 7, pp. 3412–3427, 2013.

[8] Q. Wu, G. Zhang, D. W. K. Ng, W. Chen, and R. Schober, "Generalized wireless-powered communications: When to activate wireless power transfer?" *IEEE Transactions on Vehicular Technology*, vol. 68, no. 8, pp. 8243–8248, 2019.

[9] Q. Wu, G. Y. Li, W. Chen, D. W. K. Ng, and R. Schober, "An overview of sustainable green 5g networks," *IEEE Wireless Communications*, vol. 24, pp. 72–80, 2017.

[10] R. Zhang and C. K. Ho, "Mimo broadcasting for simultaneous wireless information and power transfer," *IEEE Transactions on Wireless Communications*, vol. 12, no. 5, pp. 1989–2001, 2013.

[11] Q. Qi, X. Chen, and D. W. K. Ng, "Robust beamforming for noma-based cellular massive iot with swipt," *IEEE Transactions on Signal Processing*, vol. 68, pp. 211–224, 2019.

[12] J. Huang, C.-c. Xing, and M. Guizani, "Power allocation for d2d communications with swipt," *IEEE Transactions on Wireless Communications*, vol. 19, no. 4, pp. 2308–2320, 2020.

[13] Q. Wu, M. Tao, D. Wing Kwan Ng, W. Chen, and R. Schober, "Energy-efficient transmission for wireless powered multiuser communication networks," in *2015 IEEE International Conference on Communications (ICC)*, 2015, pp. 154–159.

[14] S. Goel and R. Negi, "Guaranteeing secrecy using artificial noise," *IEEE Transactions on Wireless Communications*, vol. 7, no. 6, pp. 2180–2189, 2008.

[15] Q. Li and W.-K. Ma, "Spatially selective artificial-noise aided transmit optimization for miso multi-eves secrecy rate maximization," *IEEE Transactions on Signal Processing*, vol. 61, no. 10, pp. 2704–2717, 2013.

[16] D. W. K. Ng, E. S. Lo, and R. Schober, "Robust beamforming for secure communication in systems with wireless information and power transfer," *IEEE Transactions on Wireless Communications*, vol. 13, no. 8, pp. 4599–4615, 2014.

[17] Y. Su and D. W. K. Ng, "Optimal beamforming for multiuser secure swipt systems (invited paper)," in *INISCOM*, 2018.

[18] D. W. K. Ng and R. Schober, "Resource allocation for secure communication in systems with wireless information and power transfer," in *2013 IEEE Globecom Workshops (GC Wkshps)*, 2013, pp. 1251–1257.

[19] D. W. K. Ng, E. S. Lo, and R. Schober, "Secure resource allocation and scheduling for ofdma decode-and-forward relay networks," *IEEE Transactions on Wireless Communications*, vol. 10, no. 10, pp. 3528–3540, 2011.

[20] S. Goel and R. Negi, "Guaranteeing secrecy using artificial noise," *IEEE transactions on wireless communications*, vol. 7, no. 6, pp. 2180–2189, 2008.

[21] B. D. Van Veen and K. M. Buckley, "Beamforming: A versatile approach to spatial filtering," *IEEE assp magazine*, vol. 5, no. 2, pp. 4–24, 1988.

[22] D. W. K. Ng and R. Schober, "Resource allocation for coordinated multipoint networks with wireless information and power transfer," in *2014 IEEE Global Communications Conference*, 2014, pp. 4281–4287.

[23] R. Meka, P. Jain, C. Caramanis, and I. S. Dhillon, "Rank minimization via online learning," in *Proceedings of the 25th International Conference on Machine Learning*, ser. ICML '08. New York, NY, USA: Association for Computing Machinery, 2008, p. 656–663. [Online]. Available: https://doi.org/10.1145/1390156.1390239

[24] D. W. K. Ng, E. S. Lo, and R. Schober, "Robust beamforming for secure communication in systems with wireless information and power transfer," *IEEE Transactions on Wireless Communications*, vol. 13, no. 8, pp. 4599–4615, 2014.

[25] J. G. Andrews, S. Buzzi, W. Choi, S. V. Hanly, A. Lozano, A. C. Soong, and J. C. Zhang, "What will 5g be?" *IEEE Journal on selected areas in communications*, vol. 32, no. 6, pp. 1065–1082, 2014.

[26] Y. Xu, G. Gui, H. Gacanin, and F. Adachi, "A survey on resource allocation for 5g heterogeneous networks: Current research, future trends, and challenges," *IEEE Communications Surveys & Tutorials*, vol. 23, no. 2, pp. 668–695, 2021.

[27] X. Chen, D. W. K. Ng, W. Yu, E. G. Larsson, N. Al-Dhahir, and R. Schober, "Massive access for 5g and beyond," *IEEE Journal on Selected Areas in Communications*, vol. 39, no. 3, pp. 615–637, 2021.

[28] A. Osseiran, F. Boccardi, V. Braun, K. Kusume, P. Marsch, M. Maternia, O. Queseth, M. Schellmann, H. Schotten, H. Taoka *et al.*, "Scenarios for 5g mobile and wireless communications: the vision of the metis project," *IEEE communications magazine*, vol. 52, no. 5, pp. 26–35, 2014.

[29] M. Agiwal, A. Roy, and N. Saxena, "Next generation 5g wireless networks: A comprehensive survey," *IEEE Communications Surveys & Tutorials*, vol. 18, no. 3, pp. 1617–1655, 2016.

[30] S. Ali, "Vehicle to vehicle communication," 06 2019.

[31] D. Niyato, E. Hossain, M. M. Rashid, and V. K. Bhargava, "Wireless sensor networks with energy harvesting technologies: A game-theoretic approach to optimal energy management," *IEEE Wireless Communications*, vol. 14, no. 4, pp. 90–96, 2007.

[32] L. Hou and S. Tan, "A preliminary study of thermal energy harvesting for industrial wireless sensor networks," in *2016 10th International Conference on Sensing Technology (ICST)*. IEEE, 2016, pp. 1–5.

[33] I. Krikidis, S. Timotheou, S. Nikolaou, G. Zheng, D. W. K. Ng, and R. Schober, "Simultaneous wireless information and power transfer in modern communication systems," *IEEE Communications Magazine*, vol. 52, no. 11, pp. 104–110, 2014.

[34] L. R. Varshney, "Transporting information and energy simultaneously," in *2008 IEEE international symposium on information theory*. IEEE, 2008, pp. 1612–1616.

[35] I.-J. Yoon, "Wireless power transfer in the radiating near-field region," in *2015 USNC-URSI Radio Science Meeting (Joint with AP-S Symposium)*. IEEE, 2015, pp. 344–344.

[36] K. Huang and X. Zhou, "Cutting the last wires for mobile communications by microwave power transfer," *IEEE Communications Magazine*, vol. 53, no. 6, pp. 86–93, 2015.

[37] X. Lu, P. Wang, D. Niyato, D. I. Kim, and Z. Han, "Wireless networks with rf energy harvesting: A contemporary survey," *IEEE Communications Surveys & Tutorials*, vol. 17, no. 2, pp. 757–789, 2014.

[38] D. A. Mindell, "Opening black's box: Rethinking feedback's myth of origin," *Technology and Culture*, vol. 41, no. 3, pp. 405–434, 2000.

[39] J. A. Paradiso and T. Starner, "Energy scavenging for mobile and wireless electronics," *IEEE Pervasive computing*, vol. 4, no. 1, pp. 18–27, 2005.

[40] L. R. Varshney and S. D. Servetto, "A distributed transmitter for the sensor reachback problem based on radar signals," in *Advances in Pervasive Computing and Networking*. Springer, 2005, pp. 227–247.

[41] B. Ananthasubramaniam and U. Madhow, "On localization performance in imaging sensor nets," *IEEE transactions on signal processing*, vol. 55, no. 10, pp. 5044–5057, 2007.

[42] Z. Wei, L. Yang, D. W. K. Ng, J. Yuan, and L. Hanzo, "On the performance gain of noma over oma in uplink communication systems," *IEEE Transactions on Communications*, vol. 68, no. 1, pp. 536–568, 2019.

[43] Z. Wei, X. Yu, D. W. K. Ng, and R. Schober, "Resource allocation for simultaneous wireless information and power transfer systems: A tutorial overview," *Proceedings of the IEEE*, 2021.

[44] J. Hu, X. Cai, and K. Yang, "Joint trajectory and scheduling design for uav aided secure backscatter communications," *IEEE Wireless Communications Letters*, vol. 9, no. 12, pp. 2168–2172, 2020.

[45] C. S. R. Murthy and B. Manoj, *Ad hoc wireless networks: Architectures and protocols, portable documents*. Pearson education, 2004.

[46] A. D. Wyner, "The wire-tap channel," *The Bell System Technical Journal*, vol. 54, no. 8, pp. 1355–1387, 1975.

[47] D. W. K. Ng and R. Schober, "Secure and green swipt in distributed antenna networks with limited backhaul capacity," *IEEE Transactions on Wireless Communications*, vol. 14, no. 9, pp. 5082–5097, 2015.

[48] X. Chen, D. W. K. Ng, W. H. Gerstacker, and H.-H. Chen, "A survey on multiple-antenna techniques for physical layer security," *IEEE Communications Surveys Tutorials*, vol. 19, no. 2, pp. 1027–1053, 2017.

[49] R. Heath, S. Peters, Y. Wang, and J. Zhang, "A current perspective on distributed antenna systems for the downlink of cellular systems," *IEEE Communications Magazine*, vol. 51, no. 4, pp. 161–167, 2013.

[50] D. Lee, H. Seo, B. Clerckx, E. Hardouin, D. Mazzarese, S. Nagata, and K. Sayana, "Coordinated multipoint transmission and reception in lte-advanced: Deployment scenarios and operational challenges," *IEEE Communications Magazine*, vol. 50, no. 2, pp. 148–155, Feb. 2012.

[51] O. Mehanna, K. Huang, B. Gopalakrishnan, A. Konar, and N. D. Sidiropoulos, "Feasible point pursuit and successive approximation of non-convex qcqps," *IEEE Signal Processing Letters*, vol. 22, no. 7, pp. 804–808, 2014.

[52] P. Jain, P. Kar *et al.*, "Non-convex optimization for machine learning," *Foundations and Trends® in Machine Learning*, vol. 10, no. 3-4, pp. 142–363, 2017.

[53] W. Yuan, C. Liu, F. Liu, S. Li, and D. W. K. Ng, "Learning-based predictive beamforming for uav communications with jittering," *IEEE Wireless Communications Letters*, vol. 9, no. 11, pp. 1970–1974, 2020.

[54] C. Liu, W. Yuan, S. Li, X. Liu, H. Li, D. W. K. Ng, and Y. Li, "Learning-based predictive beamforming for integrated sensing and communication in vehicular networks," *IEEE Journal on Selected Areas in Communications*, vol. 40, no. 8, pp. 2317–2334, 2022.

[55] C. Liu, Z. Wei, D. W. K. Ng, J. Yuan, and Y.-C. Liang, "Deep transfer learning for signal detection in ambient backscatter communications," *IEEE Transactions on Wireless Communications*, vol. 20, no. 3, pp. 1624–1638, 2021.

[56] X. Liu, C. Liu, Y. Li, B. Vucetic, and D. W. K. Ng, "Deep residual learning-assisted channel estimation in ambient backscatter communications," *IEEE Wireless Communications Letters*, vol. 10, no. 2, pp. 339–343, 2021.

[57] C. Liu, X. Liu, D. W. K. Ng, and J. Yuan, "Deep residual learning for channel estimation in intelligent reflecting surface-assisted multi-user communications," *IEEE Transactions on Wireless Communications*, vol. 21, no. 2, pp. 898–912, 2022.

[58] C. Liu, W. Yuan, Z. Wei, X. Liu, and D. W. K. Ng, “Location-aware predictive beamforming for uav communications: A deep learning approach,” *IEEE Wireless Communications Letters*, vol. 10, no. 3, pp. 668–672, 2021.

[59] C. Liu, X. Liu, S. Li, W. Yuan, and D. W. K. Ng, “Deep clstm for predictive beamforming in integrated sensing and communication-enabled vehicular networks,” *Journal of Communications and Information Networks*, vol. 7, no. 3, pp. 269–277, 2022.

[60] S. Poljak, F. Rendl, and H. Wolkowicz, “A recipe for semidefinite relaxation for (0, 1)-quadratic programming,” *Journal of Global Optimization*, vol. 7, no. 1, pp. 51–73, 1995.

[61] M. Razaviyayn, “Successive convex approximation: Analysis and applications,” Ph.D. dissertation, University of Minnesota, 2014.

[62] S. Boyd, S. P. Boyd, and L. Vandenberghe, *Convex optimization*. Cambridge university press, 2004.

[63] W. Wang, L. Yang, A. Meng, Y. Zhan, and D. W. K. Ng, “Resource allocation for irs-aided jp-comp downlink cellular networks with underlaying d2d communications,” *IEEE Transactions on Wireless Communications*, vol. 21, no. 6, pp. 4295–4309, 2022.

[64] Y. Sun, D. Xu, D. W. K. Ng, L. Dai, and R. Schober, “Optimal 3d-trajectory design and resource allocation for solar-powered uav communication systems,” *IEEE Transactions on Communications*, vol. 67, no. 6, pp. 4281–4298, 2019.

[65] Q. Wu, J. Xu, Y. Zeng, D. W. K. Ng, N. Al-Dhahir, R. Schober, and A. L. Swindlehurst, “A comprehensive overview on 5g-and-beyond networks with uavs: From communications to sensing and intelligence,” *IEEE Journal on Selected Areas in Communications*, 2021.

[66] Y. Cai, Z. Wei, R. Li, D. W. K. Ng, and J. Yuan, “Joint trajectory and resource allocation design for energy-efficient secure uav communication systems,” *IEEE Transactions on Communications*, vol. 68, no. 7, pp. 4536–4553, 2020.

[67] Q. Wu, J. Xu, Y. Zeng, D. W. K. Ng, N. Al-Dhahir, R. Schober, and A. L. Swindlehurst, “A comprehensive overview on 5g-and-beyond networks with uavs: From communications to sensing and intelligence,” *IEEE Journal on Selected Areas in Communications*, vol. 39, no. 10, pp. 2912–2945, 2021.

[68] Y. Cai, Z. Wei, S. Hu, C. Liu, D. W. K. Ng, and J. Yuan, "Resource allocation and 3d trajectory design for power-efficient irs-assisted uav-noma communications," *IEEE Transactions on Wireless Communications*, pp. 1–1, 2022.

[69] X. Yu, D. Xu, D. W. K. Ng, and R. Schober, "Irs-assisted green communication systems: Provable convergence and robust optimization," *IEEE Transactions on Communications*, vol. 69, no. 9, pp. 6313–6329, 2021.

[70] X. Yu, D. Xu, Y. Sun, D. W. K. Ng, and R. Schober, "Robust and secure wireless communications via intelligent reflecting surfaces," *IEEE Journal on Selected Areas in Communications*, vol. 38, no. 11, pp. 2637–2652, 2020.

[71] X. Yu, D. Xu, D. W. K. Ng, and R. Schober, "Irs-assisted green communication systems: Provable convergence and robust optimization," *IEEE Transactions on Communications*, vol. 69, no. 9, pp. 6313–6329, 2021.

[72] S. Hu, Z. Wei, Y. Cai, C. Liu, D. W. K. Ng, and J. Yuan, "Robust and secure sum-rate maximization for multiuser miso downlink systems with self-sustainable irs," *IEEE Transactions on Communications*, vol. 69, no. 10, pp. 7032–7049, 2021.

[73] X. Yu, V. Jamali, D. Xu, D. W. K. Ng, and R. Schober, "Smart and reconfigurable wireless communications: From irs modeling to algorithm design," *IEEE Wireless Communications*, vol. 28, no. 6, pp. 118–125, 2021.

Appendix 1

Proof of Theorem 1 :

We can notice that P4 is jointly convex after using rank relaxation and satisfies the Slaters condition so that the strong duality holds. As a result, the dual problem's solution will be the same as the relaxation problem's solution, or the gap between the two solutions will be zero. To solve the duality problem, the Lagrangian function is written as :

$$
\begin{aligned}
\mathcal{L} = & \sum_{k=1}^{K} \xi_k \left(\gamma_k \left(\sum_{j \neq k}^{K} \left\| \mathbf{h}_k \bar{\mathbf{W}}_j \mathbf{h}_k^H \right\|^2 + \mathrm{Tr}\left(\mathbf{H}_k \mathbf{V}\right) + \sigma_k^2 \right) - \left\| \mathbf{h}_k \bar{\mathbf{W}}_k \mathbf{h}_k^H \right\|^2 \right) && (1) \\
& + \sum_{k=1}^{K} \vartheta_k \left(\eta \left\| \mathbf{g}_m \bar{\mathbf{W}}_k \mathbf{g}_m^H \right\|^2 - \Gamma_{th} \left(\eta \sum_{j \neq k}^{K} \left\| \mathbf{g}_m \bar{\mathbf{W}}_j \mathbf{g}_m^H \right\|^2 + \mathrm{Tr}\left(\mathbf{G}_m \mathbf{V}\right) + \sigma_k^2 \right) \right) && (2) \\
& + \sum_{k=1}^{K} \nu_k \left(\left\| \mathbf{q}_n \bar{\mathbf{W}}_k \mathbf{q}_n^H \right\|^2 - \Gamma_{th} \left(\sum_{j \neq k}^{K} \left\| \mathbf{q}_n \bar{\mathbf{W}}_j \mathbf{q}_n^H \right\|^2 + \mathrm{Tr}\left(\mathbf{Q}_m \mathbf{V}\right) + \sigma_k^2 \right) \right) && (3) \\
& + \sum_{l=1}^{L} \omega_k \left(\sum_{k=1}^{K} \mathrm{Tr}\left(\bar{\mathbf{W}}_{l,k}\right) - P_{max} \right) && (4) \\
& + \sum_{k=1}^{K} \zeta_k \left(\sum_{k=1}^{K} \left\| \mathbf{h}_k \bar{\mathbf{W}}_k \mathbf{h}_k^H \right\|^2 + \mathrm{Tr}(\mathbf{H}_k \mathbf{V}) + \sigma_s^2 - \varphi_k \right) && (5) \\
& + \sum_{k=1}^{K} \Phi_k \left(\delta_k - \sum_{j \neq k}^{K} \left\| \mathbf{h}_k \bar{\mathbf{W}}_j \mathbf{h}_k^H \right\|^2 - \mathrm{Tr}(\mathbf{H}_k \mathbf{V}) - \sigma_s^2 \right) && (6) \\
& - \sum_{n=1}^{N} \sum_{k=1}^{K} \mathrm{Tr}\left(\bar{\mathbf{W}}_{l,k} \mathbf{Y}_{l,k}\right) + \Theta && (7)
\end{aligned}
$$

In order to simplify this function, the items that do not contain $\bar{\mathbf{W}}_{l,k}$ are uniformly replaced by Λ, and the original formula is rewritten as :

$$\mathcal{L}=\sum_{k=1}^{K}\xi_k\left(\gamma_k\sum_{j\neq k}^{K}\left\|\mathbf{h}_k\bar{\mathbf{W}}_j\mathbf{h}_k^H\right\|^2-\left\|\mathbf{h}_k\bar{\mathbf{W}}_k\mathbf{h}_k^H\right\|^2\right) \tag{8}$$

$$+\sum_{k=1}^{K}\vartheta_k\left(\eta\left\|\mathbf{g}_m\bar{\mathbf{W}}_k\mathbf{g}_m^H\right\|^2-\eta\Gamma_{th}\sum_{j\neq k}^{K}\left\|\mathbf{g}_m\bar{\mathbf{W}}_j\mathbf{g}_m^H\right\|^2\right) \tag{9}$$

$$+\sum_{k=1}^{K}\nu_k\left(\left\|\mathbf{q}_n\bar{\mathbf{W}}_k\mathbf{q}_n^H\right\|^2-\Gamma_{th}\sum_{j\neq k}^{K}\left\|\mathbf{q}_n\bar{\mathbf{W}}_j\mathbf{q}_n^H\right\|^2\right) \tag{10}$$

$$+\sum_{l=1}^{L}\omega_k\sum_{k=1}^{K}\mathrm{Tr}\left(\bar{\mathbf{W}}_{l,k}\right) \tag{11}$$

$$+\sum_{k=1}^{K}\zeta_k\sum_{k=1}^{K}\left\|\mathbf{h}_k\bar{\mathbf{W}}_k\mathbf{h}_k^H\right\|^2 \tag{12}$$

$$-\sum_{k=1}^{K}\Phi_k\sum_{j\neq k}^{K}\left\|\mathbf{h}_k\bar{\mathbf{W}}_j\mathbf{h}_k^H\right\|^2 \tag{13}$$

$$-\sum_{n=1}^{N}\sum_{k=1}^{K}\mathrm{Tr}\left(\bar{\mathbf{W}}_{l,k}\mathbf{Y}_{l,k}\right)+\Lambda \tag{14}$$

Next we reveal the structure of the optimal solution of $\bar{\mathbf{W}}_{l,k}^{\star}$by examining the KKT conditions, given by :

$$\mathrm{K1}:\xi_k^{\star},\vartheta_k^{\star},\nu_k^{\star},\omega_l^{\star},\zeta_k^{\star},\Phi_k^{\star}\geq 0,\quad \mathrm{Y}_{l,k}^{\star}\succeq 0, \tag{15}$$

$$\mathrm{K2}:\mathbf{Y}_{l,k}^{\star}\bar{\mathbf{W}}_{l,k}^{\star}=0, \tag{16}$$

$$\mathrm{K3}:\bigtriangledown_{\bar{\mathbf{W}}_{l,k}}\mathcal{L}\left(\bar{\mathbf{W}}_{l,k}^{\star}\right)=0, \tag{17}$$

$\xi_k^{\star},\vartheta_k^{\star},\nu_k^{\star},\omega_l^{\star},\zeta_k^{\star},\Phi_k^{\star},$and $\mathrm{Y}_{l,k}^{\star}$ are the optimal Lagrange multipliers of the dual problem. $\bigtriangledown_{\bar{\mathbf{W}}_{l,k}}\mathcal{L}\left(\bar{\mathbf{W}}_{l,k}^{\star}\right)$ represents the gradient of the Lagrangian function, and then K3 can be rewritten as the following form.

$$\mathrm{Y}_{l,k}^{\star}=\omega_l^{\star}\mathrm{I}_{L_t}-\Xi_{l,k}^{\star} \tag{18}$$

$\Xi_{l,k}^{\star}$ is an expression for $\bar{\mathbf{W}}_{l,k}^{\star}$, which is written as :

$$\Xi_{l,k}^{\star} = \xi_k^{\star}\mathbf{h}_{l,k}^{H}\mathbf{h}_{l,k}\bar{\mathbf{W}}_{l,k}\mathbf{h}_{l,k}^{H}\mathbf{h}_{l,k} - \sum_{j\neq k}^{K}\xi_j^{\star}\gamma_j\mathbf{h}_{l,k}^{H}\mathbf{h}_{l,k}\bar{\mathbf{W}}_{l,j}\mathbf{h}_{l,k}^{H}\mathbf{h}_{l,k} \tag{19}$$

$$+ \sum_{j\neq k}^{K}\vartheta_j^{\star}\eta\Gamma_{th}\mathbf{g}_{l,m}^{H}\mathbf{g}_{l,m}\bar{\mathbf{W}}_{l,j}\mathbf{g}_{l,m}^{H}\mathbf{g}_{l,m} - \vartheta_k^{\star}\eta\mathbf{g}_{l,m}^{H}\mathbf{g}_{l,m}\bar{\mathbf{W}}_{l,k}\mathbf{g}_{l,m}^{H}\mathbf{g}_{l,m} \tag{20}$$

$$+ \sum_{j\neq k}^{K}\nu_j^{\star}\Gamma_{th}\mathbf{q}_{l,n}^{H}\mathbf{q}_{l,n}\bar{\mathbf{W}}_{l,j}\mathbf{q}_{l,n}^{H}\mathbf{q}_{l,n} - \nu_k^{\star}\mathbf{q}_{l,n}^{H}\mathbf{q}_{l,n}\bar{\mathbf{W}}_{l,k}\mathbf{q}_{l,n}^{H}\mathbf{q}_{l,n} \tag{21}$$

$$- \sum_{k=1}^{K}\zeta_k^{\star}\mathbf{h}_{l,k}^{H}\mathbf{h}_{l,k}\bar{\mathbf{W}}_{l,k}\mathbf{h}_{l,k}^{H}\mathbf{h}_{l,k} + \sum_{j\neq k}^{K}\Phi_j^{\star}\mathbf{h}_{l,k}^{H}\mathbf{h}_{l,k}\bar{\mathbf{W}}_{l,j}\mathbf{h}_{l,k}^{H}\mathbf{h}_{l,k} \tag{22}$$

The optimal solution $\bar{\mathbf{W}}_{l,k}^{\star}$ always satisfies Rank $\left(\bar{\mathbf{W}}_{l,k}^{\star}\right) = 1$ will be proved by analyzing the structure of $\Upsilon_{l,k}^{\star}$. The first step is to prove by contradiction that $\Xi_{l,k}^{\star}$ is a positive semi-definite matrix. Defined the maximum eigenvalue of $\Xi_{l,k}^{\star}$ as $\lambda_{\max}\left(\Xi_{l,k}^{\star}\right)$. Assuming $\lambda_{\max}\left(\Xi_{l,k}^{\star}\right) < 0$, $\Upsilon_{l,k}^{\star}$ will be a full rank matrix, which leads to $\bar{\mathbf{W}}_{l,k}^{\star} = 0$, this would contradict with $\omega_l^{\star} > 0$ in KKT condition K1 and $P_{\max} > 0$. Hence, we discuss the case when $\Xi_{l,k}^{\star}$ is a positive semi-definite matrix. Secondly, if $\omega_l^{\star} < \lambda_{\max}\left(\Xi_{l,k}^{\star}\right)$, the condition that $\Upsilon_{l,k}^{\star}\Upsilon$ is a positive definite matrix is not guaranteed. However, if $\omega_l^{\star} > \lambda_{\max}\left(\Xi_{l,k}^{\star}\right)$, $\Xi_{l,k}^{\star}$ will be a positive semi-definite matrix, which also contradict with $\omega_l^{\star} > 0$ in KKT condition K1 and $P_{\max} > 0$. According to the above proof, there is only one possibility, that is $\omega_l^{\star} = \lambda_{\max}\left(\Xi_{l,k}^{\star}\right)$, such that $\Upsilon_{l,k}^{\star}\lambda_{\max}\left(\Xi_{l,k}^{\star}\right) = 0$. Therefore, the optimal solution $\bar{\mathbf{W}}_{l,k}^{\star}$ always satisfies the Rank $\left(\bar{\mathbf{W}}_{l,k}^{\star}\right) = 1$.